Appendix 1

Federated States of Micronesia—Climate Risk Profile

Summary

The likelihood (i.e., probability) components of climate-related risks in the Federated States of Micronesia (FSM) are evaluated, for both present-day and future conditions. Changes over time reflect the influence of global warming.

The risks evaluated are extreme rainfall events (both hourly and daily), drought, high sea levels, strong winds, and extreme high air temperatures.

Projections of future climate-related risk are based on the output of global climate models, for given emission scenarios and model sensitivity.

With the exception of maximum wind speed, projections of all the likelihood components of climate-related risk show marked increases as a result of global warming.

A. Introduction

Formally, risk is the product of the consequence of an event or happening and the likelihood (i.e., probability) of that event taking place.

While the consequence component of a climate-related risk will be site or sector specific, in general the likelihood component of a climate-related risk will be applicable over a larger geographical area and to many sectors. This is due to the spatial scale and pervasive nature of weather and climate. Thus the likelihood of, say, an extreme event or climate anomaly is often evaluated for a country, state, small island, or similar geographical unit. While the likelihood may well be within a given unit, information is often insufficient to assess this spatial variability, or the variations are judged to be of low practical significance.

The following climate conditions are considered to be among the potential sources of risk:

- extreme rainfall events,
- drought,
- high sea levels,
- strong winds, and
- extreme high air temperatures.

B. Methods

Preparation of a climate risk profile for a given geographical unit involves an evaluation of current likelihoods of all relevant climate-related risks, based on observed and other pertinent data.

Climate change scenarios are used to develop projections of how the likelihoods might change in the future. For rainfall and temperature projections, the Hadley Centre (United Kingdom) global climate model (GCM) was used, as it gave results intermediate between those provided by three other GCMs, namely those developed by the Australian Commonwealth Scientific and Industrial Research Organisation, Japan's National Institute for Environmental Science, and the Canadian Climate Centre. For drought, strong winds, and sea level, the Canadian GCM was used to develop projections.

Similarly, the SRES A1B greenhouse gas emission scenario was used when preparing rainfall, temperature, and sea level projections. Figure A1.1 shows that this scenario is close to the middle of the envelope of projected emissions and greenhouse

gas concentrations. For drought both the A2 and B2 emission scenarios were used, while for strong winds only the A2 scenario was used.

Figure A1.1. Scenarios of CO_2 Gas Emissions and Consequent Atmospheric Concentrations of CO_2

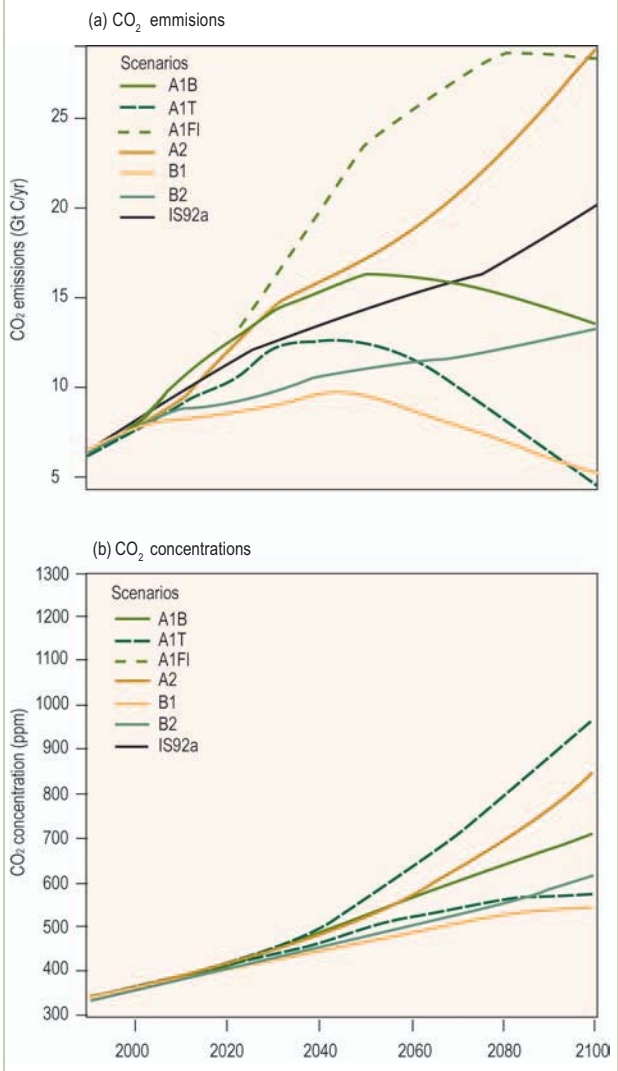

Notes: CO_2 = carbon dioxide; Gt C/yr = gigatonnes of carbon per year.
Source: IPCC 2001.

C. Information Sources

Daily and hourly rainfall, daily temperatures, and hourly wind data were obtained through the Pohnpei Weather Service Office and with the assistance of Mr. Chip Guard, National Oceanic and Atmospheric Administration, Guam. Sea-level data for Pohnpei were supplied by the National Tidal Facility, The Flinders University of South Australia, and are copyright reserved. The sea-level data derived from Topex-Poisidon satellite observations were obtained from www.//podaac-esip.jpl.nasa.gov.

D. Data Specifications

While much of the original data was reported in Imperial units, all data are presented using System International units.

E. Uncertainties

The sources of uncertainty in projections of the likelihood components of climate-related risks are numerous. They include uncertainties in greenhouse gas emissions and those arising from modeling the complex interactions and responses of the atmospheric and ocean systems. Figure A1.2 shows how uncertainties in greenhouse gas emissions impact on estimates of the return periods of a daily precipitation of at least 250 mm for Pohnpei.

Similar graphs can be prepared for other GCMs and extreme events, but are not shown here. Policy and decision makers need to be cognizant of uncertainties in projections of the likelihood components of extreme events.

F. Graphical Presentations

Many of the graphs that follow portray the likelihood of a given extreme event as a function of a time horizon. This is the most appropriate and useful way in which to depict risk since design life (i.e., time horizon) varies depending on the nature of the infrastructure or other development project.

Figure A1.2. Return Periods for Daily Rainfall of 250 mm in Pohnpei for Given Greenhouse Gas Emission Scenarios

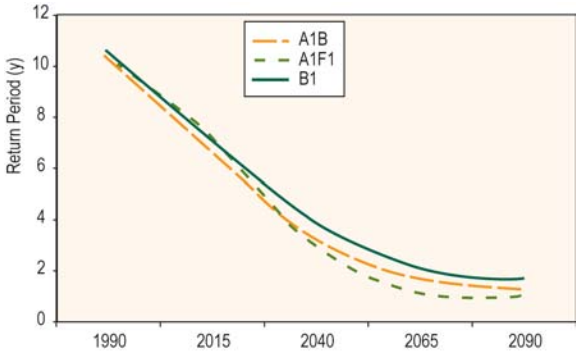

Note: Calculations used Hadley Center GCM with Best Judgment of Sensitivity.
Source: CCAIRR findings.

G. Extreme Rainfall Events

Daily Rainfall

Figure A1.3 shows the frequency distribution of daily precipitation for Pohnpei. A daily total above 250 mm is a relatively rare event, with a return period (i.e., recurrence interval) of 10 years.

Figure A1.4 shows the likelihood of such an extreme rainfall event occurring in Pohnpei and Kosrae, within a given time horizon ranging from 1 to 50 years.

As shown in Table A1.1, global warming will significantly alter the return periods, and hence the likelihoods, of the extreme rainfall events. For example, Figure A1.5 illustrates how the likelihood of a daily rainfall of 250 mm will increase over the remainder of the present century.

Figure A1.3. Frequency Distribution of Daily Precipitation for Pohnpei
(1953–2003)

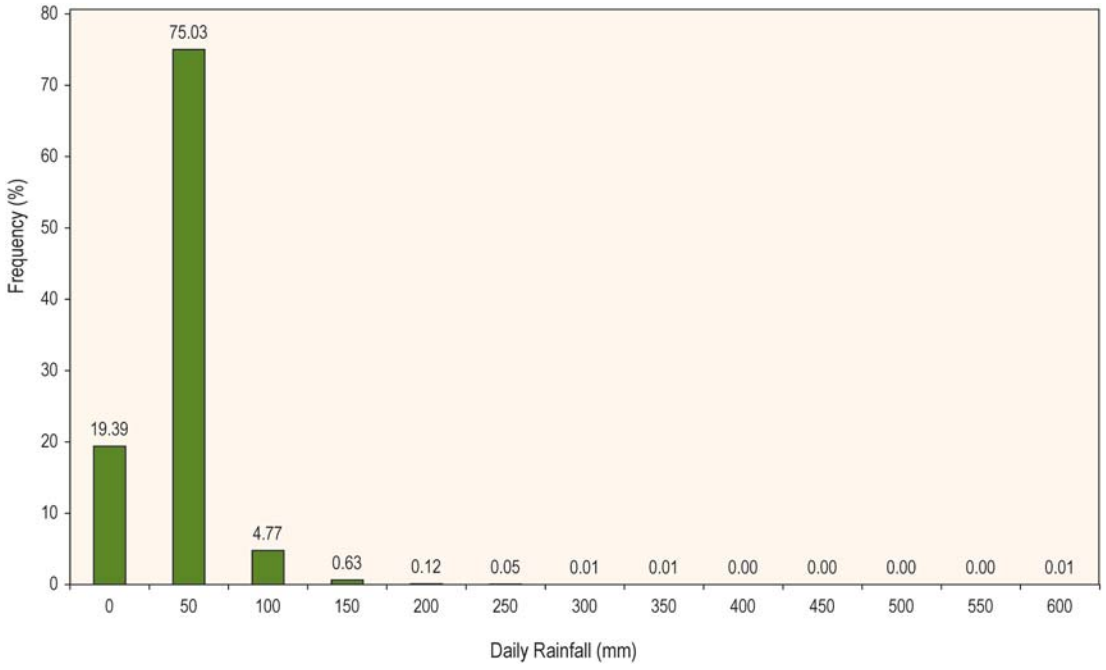

mm = millimeters.
Note: The numbers above the bars represent the frequency of occurrence, in percentages, for the given data interval.
Source: CCAIRR findings.

Figure A1.4. Return Periods for a Daily Rainfall of 250 mm Occurring Within the Indicated Time Horizon
(years)

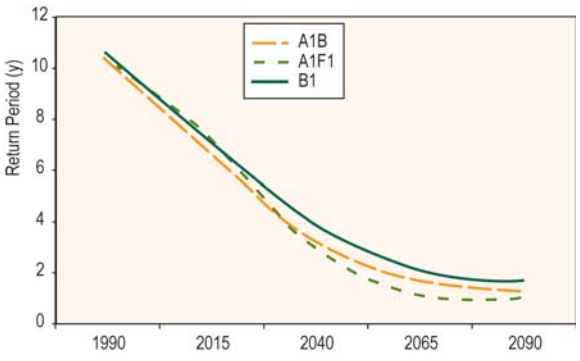

Note: 0 = zero chance; 1 = statistical certainty.

Data are for Pohnpei (1953–2003) and Kosrae (1953–2001, with gaps). A daily rainfall of 250 mm has a return period of 10 and 16 years, respectively.

Source: CCAIRR findings.

Figure A1.5. Likelihood of a Daily Rainfall of 250 mm Occurring Within the Indicated Time Horizon
(years)

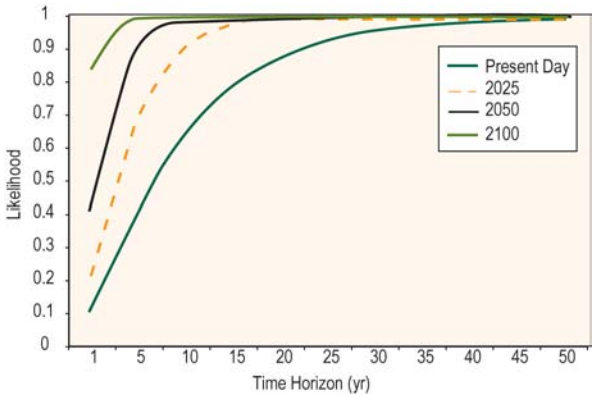

Note: 0 = zero chance; 1 = statistical certainty.
Data are for Pohnpei.

Source: CCAIRR findings.

Table A1.1: Return Periods for Daily Rainfall, Pohnpei and Kosrae

(years)

Rainfall (mm)	Present	2025	2050	2100
Pohnpei				
100	1	1	1	1
150	2	1	1	1
200	5	2	1	1
250	10	5	2	1
300	21	9	4	2
350	40	17	8	2
400	71	28	13	3
450	118	45	20	5
500	188	68	30	7
Kosrae				
100	1	1	1	1
150	3	2	1	1
200	6	4	2	2
250	16	9	5	2
300	38	21	12	4
350	83	50	31	9
400	174	119	83	22
450	344	278	237	64
00	652	632	410	230

Source: CCAIRR findings.

Hourly Rainfall

Figure A1.6 shows the frequency distribution of hourly precipitation for Pohnpei. An hourly total above 100 mm (3.9 in) is a relatively rare event. Table A1.2 shows that such a rainfall has a return period of 6 years. The table also shows, for both Pohnpei and Kosrae, that global warming will have a significant impact on the return periods of extreme rainfall events.

Figure A1.7 depicts the impact of global warming on the likelihood of an hourly rainfall of 200 mm for Pohnpei.

H. Drought

Figure A1.8 presents, for Pohnpei, the number of months in each year (1953–2003) and each decade for which the observed precipitation was below the fifth percentile. Monthly rainfall below the fifth percentile is used here as an indicator of drought.

Most of the low rainfall months are concentrated in the latter part of the period of observation, indicating that the frequency of drought has increased since the 1950s. The years with a high

Figure A1.6. Frequency Distribution of Hourly Precipitation for Pohnpei

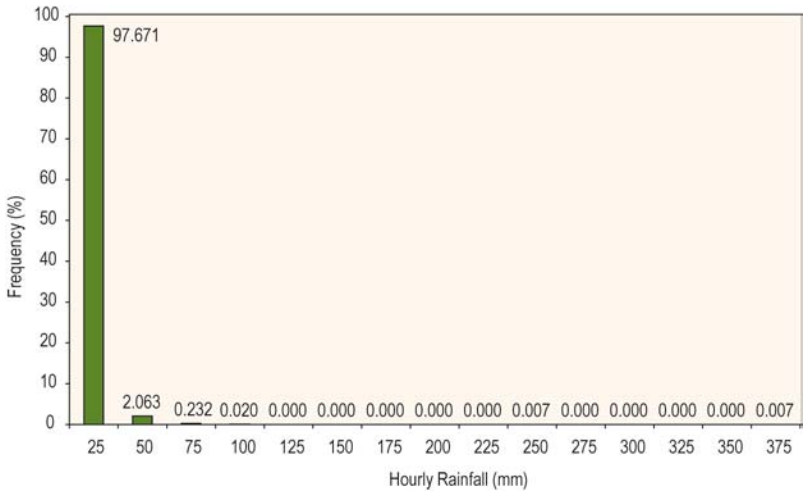

Notes: Data are for 1980 to 2002, with gaps. The numbers above the bars represent the frequency of occurrence for the given data interval, in percent of hours of observed rainfall.

Source: CCAIRR findings.

Table A1.2: Return Periods for Hourly Rainfall, Pohnpei and Kosrae

(years)

Rainfall (mm)	Present	2025	2050	2100
Pohnpei				
50	2	1	1	1
100	6	3	2	1
150	14	7	4	2
200	23	12	7	4
250	34	18	11	5
300	47	25	15	8
350	61	32	20	10
400	77	40	26	13
Kosrae				
50	2	2	1	1
100	8	6	5	3
150	16	13	10	6
200	28	21	16	11
250	41	31	24	16
300	56	42	33	22
350	73	55	43	29
400	91	68	54	37

Source: CCAIRR findings.

Figure A1.7. Likelihood of an Hourly Rainfall of 200 mm Occurring in Pohnpei Within the Indicated Time Horizon

(years)

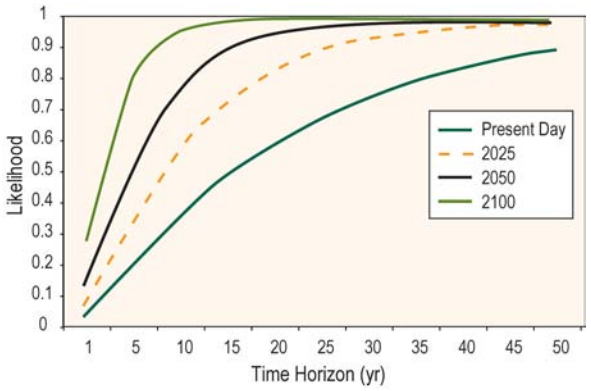

Notes: 0 = zero chance; 1 – statistical certainty. Values for present day based on observed data for 1980–2002, with gaps.

Source: CCAIRR findings.

Figure A1.8. Number of Months in Each Year or Decade for Which the Precipitation Was Below the Fifth Percentile

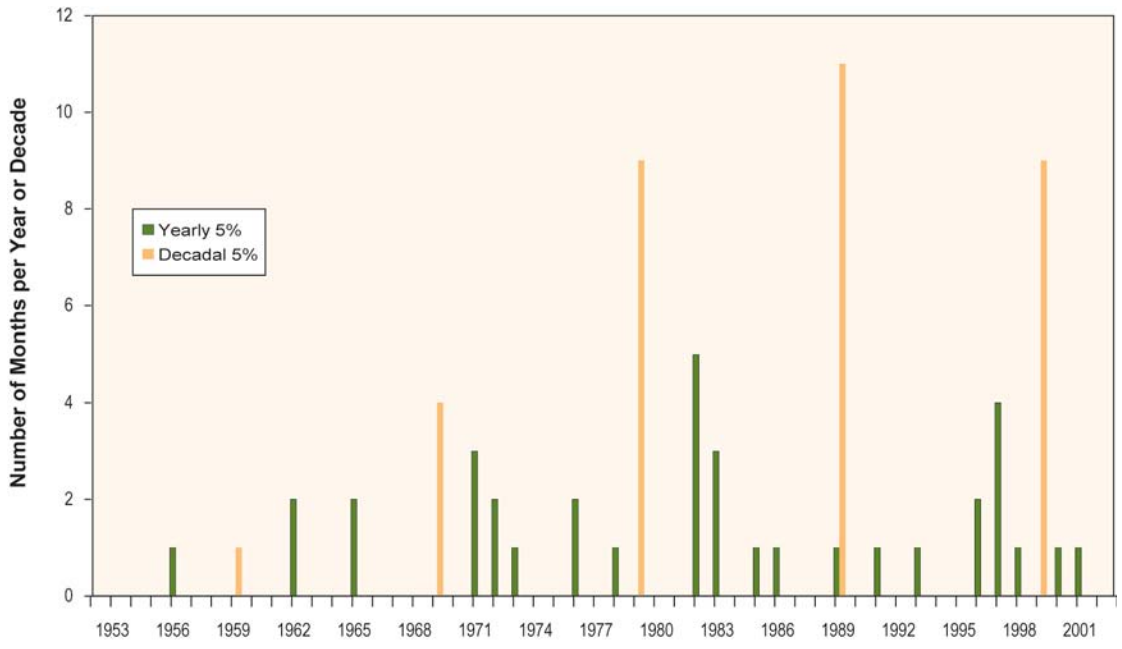

Note: Data are for Pohnpei.
Source: CCAIRR findings.

number of months below the fifth percentile coincide with El Niño Southern Oscillation (ENSO) events.

A similar analysis could not be undertaken for Kosrae, because its rainfall records are incomplete.

Figure A1.9 shows the results of a similar analysis, but for rainfall estimates (1961–1990) and projections (1991–2100) by the Canadian GCM. The results are presented for both the A2 and B2 emission scenarios.

Figure A1.9 also shows that the GCM replicates the increased frequency of months with extreme low rainfall during the latter part of the last century. The results also indicate that, regardless of which emission scenario is used, the frequency of low rainfall months will generally remain high relative to the latter part of the last century.

I. High Sea Levels

Figure A1.10 shows daily mean values of sea level for Pohnpei, relative to mean sea level. Large interannual variability occurs in sea level. Low sea levels are associated with El Niño events, while exceptionally high sea levels occurred in October 1988.

Even more extreme high sea levels occur over time scales of less than a day. Table A1.3 provides return periods for given sea level elevations for Pohnpei, for the present day and projected future. The latter projections are based on the Canadian GCM 1 GS and the A1B emission scenario.

Figure A1.9. Number of Months per Decade for Which Pecipitation for Pohnpei is Projected to be Below the Fifth Percentile

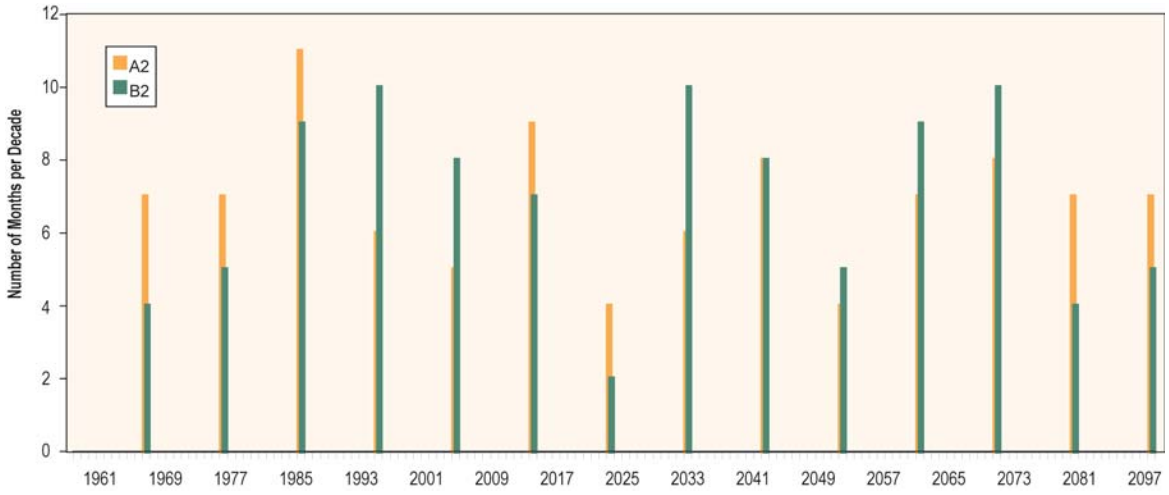

Note: data from the Canadian Global Climate Model, with A2 and B2 emission scenarios and best estimate for GCM sensitivity.
Source: CCAIRR findings.

Figure A1.10: Daily Mean Values of Sea Level for Pohnpei
(1974–2003)

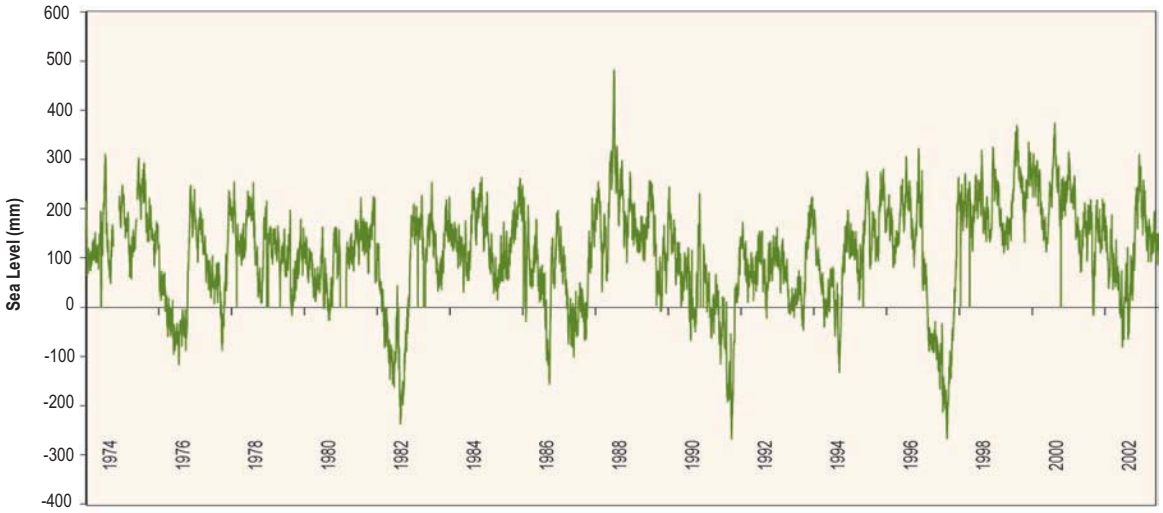

Note: The sea level elevations are relative to surveyed mean sea level.
Source: CCAIRR findings.

Table A1.3. Return Periods for Extreme High Sea Levels, Pohnpei
(years)

Sea Level (mm)	Present Day	2025	2050	2100
80	1	1	1	1
90	1	1	1	1
100	4	2	1	1
110	14	5	2	1
120	61	21	5	1
130	262	93	20	1
140	1,149	403	86	2

Note: cm = centimeters.
Source: CCAIRR findings.

The indicated increases in sea level over the next century are driven by global and regional changes in mean sea level as a consequence of global warming. Figure A1.11 illustrates the magnitude of this contribution.

Sea level elevations are not recorded *in situ* for Kosrae. However, satellite observations of sea levels are available and can add some understanding to both historic and anticipated changes in sea levels.

Figure A1.11 Sea-Level Projections for Pohnpei, Based on the Canadian GCM 1GS and the A1B Emission Scenario

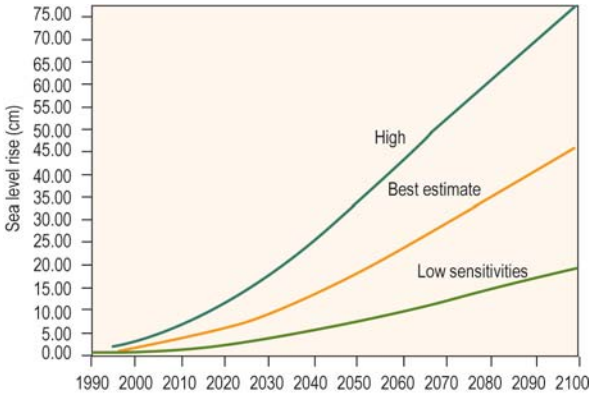

cm = centimeters; GCM = global climate model. Uncertainties related to GCM sensitivity are indicated by the blue, red, and green lines, representing high, best estimate, and low sensitivities, respectively.
Source: CCAIRR findings.

A high level of agreement occurs between the tide gauge and satellite measurements of sea level, at least for monthly averaged data (Figure A1.12).

Figure A1.12. Sea Level (departure from normal) as Determined by the Pohnpei Tide Gauge and by Satellite

rms = root mean square.
Source: CCAIRR findings..

Figure A1.13. Five-Day Mean Values of Satellite-Based Estimates of Sea Level for a Grid Square Centered on Kosrae (5.25° to 5.37°N; 162.88° to 163.04°E)

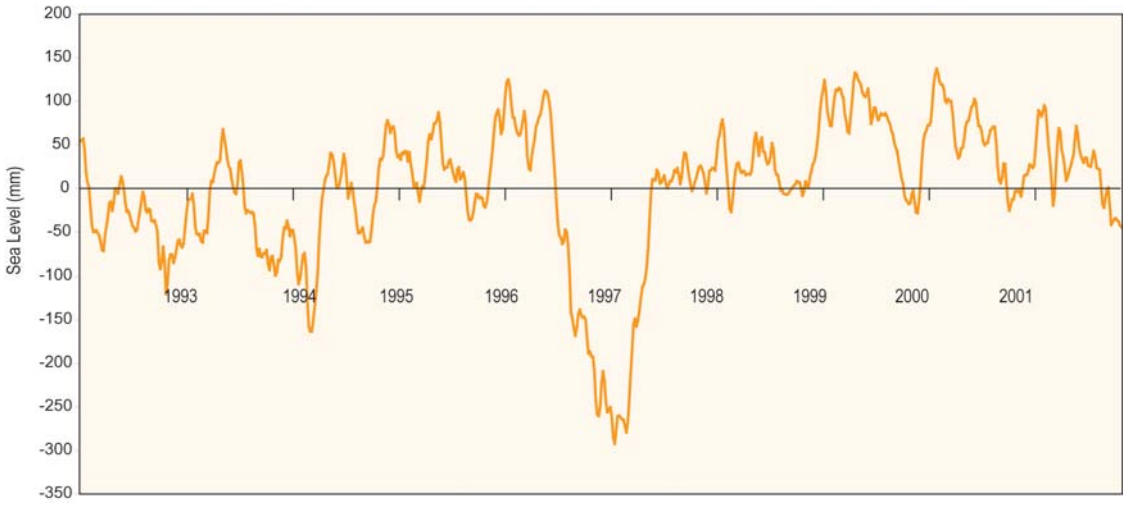

Note: Values are departures from the mean for the period of record: November 1992–August 2002.
Source: CCAIRR findings.

This reinforces confidence in the use of satellite data to characterize sea level for Kosrae. Figure A1.13 presents satellite-based estimates of sea level for a grid square centred on Kosrae.

Figure A1.14 presents the projected increase in sea level for Kosrae as a consequence of global warming. The global and regional components of sea-level rise for Kosrae are very similar to those for Pohnpei.

J. Strong Winds

Figure A1.15 shows the annual maximum wind gust recorded in Pohnpei for the period 1974–2003.

Table A1.4 presents return periods for extreme high winds in Pohnpei, based on observed data. Also shown are return periods for 1990–2020 and for 2021–2050. The latter are estimated from projections of maximum wind speed using the Canadian GCM 2 with the A2 emission scenario.

Figure A1.14. Sea-Level Projections for Kosrae, Based on the Canadian GCM 1 GS and the A1B Emission Scenario

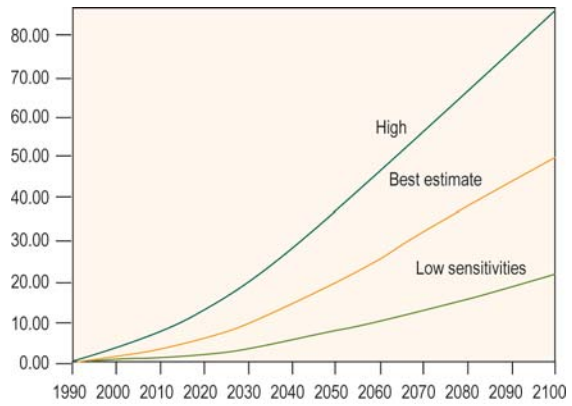

cm = centimeters; GCM = global climate model. Uncertainties related to GCM sensitivity are indicated by the blue, red, and green lines, representing high, best estimate, and low sensitivities, respectively.
Source: CCAIRR findings.

Figure 1.15. Annual Maximum Wind Gust Recorded in Pohnpei for the Period 1974–2003

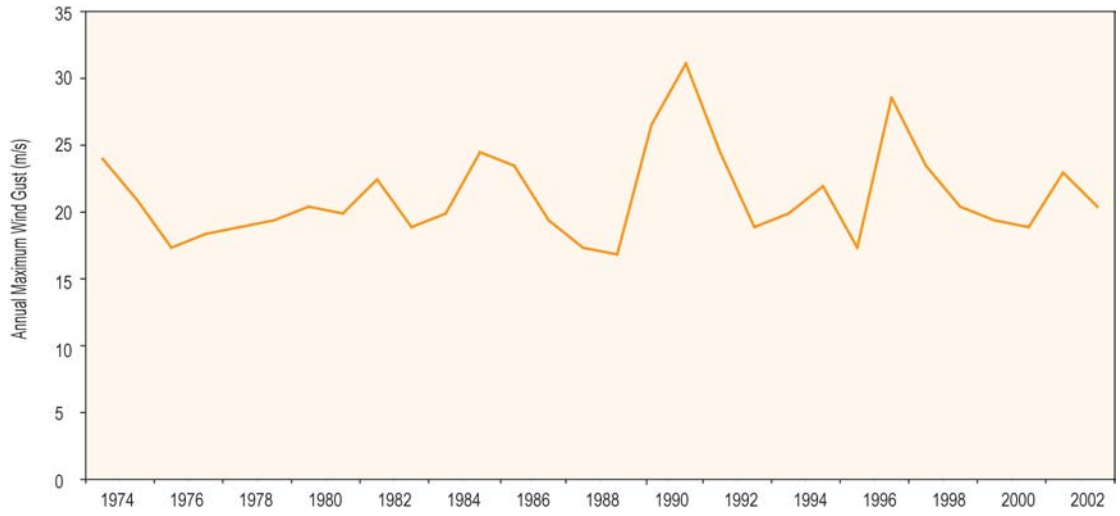

Note: m/s = meters per second.
Source: CCAIRR findings.

Table A1.4. Return Periods for Maximum Wind Speed, Pohnpei
(years)

Wind Speed (m^{s-1})	Hourly	Daily		
	1974–2003	1961–1990	1991–2020	2021–2050
20	2	2	2	2
25	8	10	10	9
28	20	47	40	20

Source: CCAIRR findings.

Figure A1.16 depicts the impact of global warming on the likelihood of a maximum wind gust of 28 m^{s-1} for Pohnpei.

Figure A1.16 Likelihood of a Maximum Wind Gust of 28 m^{s-1} Occurring Within the Indicated Time Horizon in Pohnpei
(years)

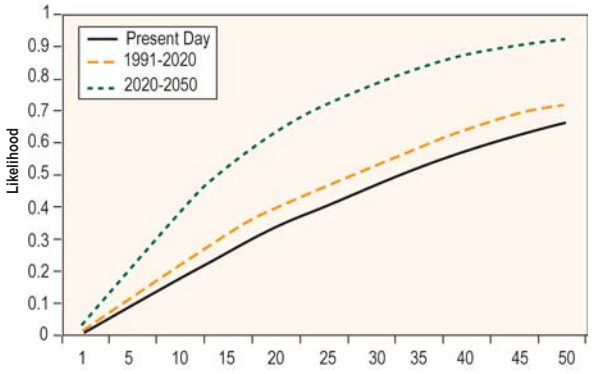

0 = zero chance; 1 – statistical certainty.

Note: Values based on Canadian Global Climate Model 2, with A2 emission scenario.
Source: CCAIRR findings.

K. Extreme High Temperatures

Figure A1.17 presents the frequency distribution of daily maximum temperature for Pohnpei.

Figure A1.17. Frequency Distribution of Daily Maximum Temperature for Pohnpei

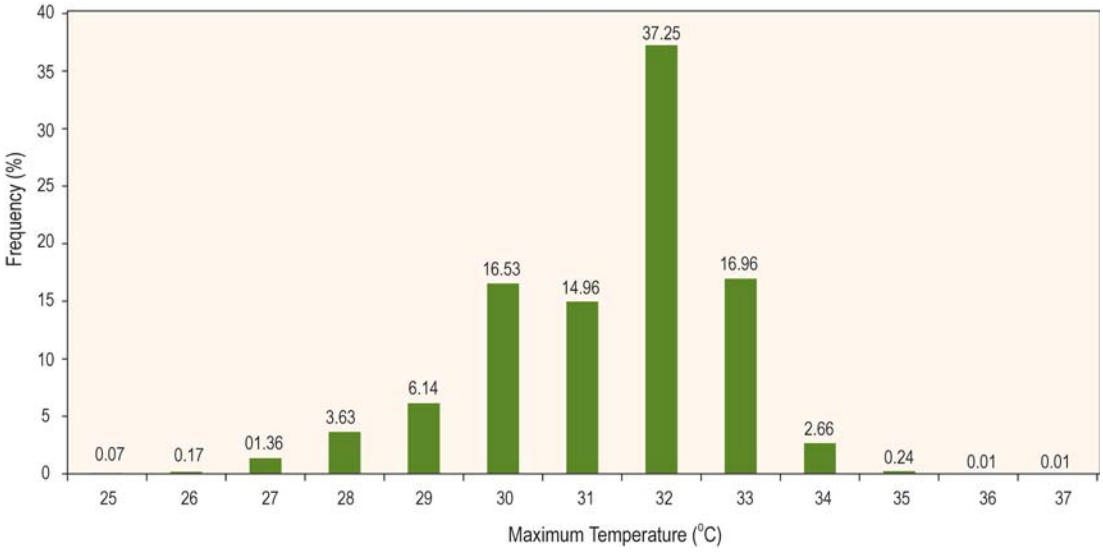

Source: Based on observed data 1953–2001.

Table A1.5 details the return periods for daily maximum temperature for Pohnpei, based on observed data (1953–2001) and projections using the Hadley Centre GCM and the A1B emission scenario.

Figure A1.18 depicts the impact of global warming on the likelihood of a daily maximum temperature of 36°C for Pohnpei.

Table A1.5. Return Periods for Daily Maximum Temperature, Pohnpei
(years)

Maximum Temperature (°C)	Observed (1953–2001)	Projected 2025	Projected 2050	Projected 2100
32	1	1	1	1
33	1	1	1	1
34	4	2	2	1
35	24	11	6	2
36	197	80	39	10
37	2,617	1,103	507	101

Source: CCAIRR findings.

Figure A1.18. Likelihood of a Maximum Temperature of 36°C Occurring Within the Indicated Time Horizon in Pohnpei
(years)

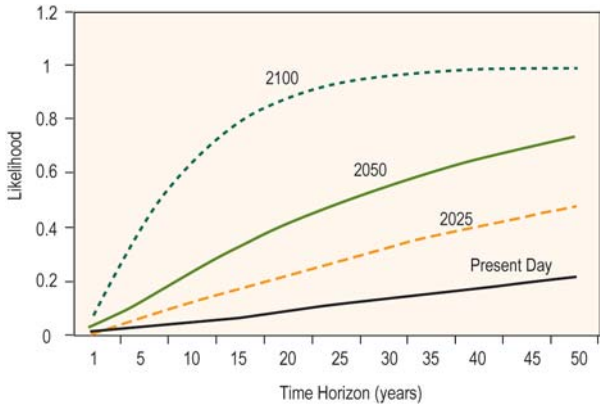

Likelihood 0 = zero chance; 1 – statistical certainty.
Notes: Values based on observed data (1953–2001) and on projections from the Hadley Centre Global Climate Module (GCM) with A1B emission scenario and best estimate of GCM sensitivity.
Source: CCAIRR findings.